

Xenon $4p$ photoionization near the $4d$ Cooper minimum: Interchannel coupling effects

N. Shanthi and P. C. Deshmukh

Department of Physics, Indian Institute of Technology, Madras 600 036, India

(Received 26 April 1989)

Recently, results of photoemission measurements for xenon were reported in the photon energy range 160 to 270 eV. These time-of-flight studies performed by Lindle *et al.* [Phys. Rev. A **37**, 3808 (1988)] at the Stanford Synchrotron Radiation Laboratory suggested that photoemission from the Xe $4p$ subshell is remarkably influenced by photoionization channels from the $4d$ subshell. In the present study, calculations in the relativistic random-phase approximation have been made in which we have included interchannel coupling between dipole photoionization channels from the $4p$ and $4d$ subshells. The effect of this interchannel coupling is perceptible in the results for $4p$ photoionization.

I. INTRODUCTION

The breakdown of the one-electron model in the description of photoelectron and related processes in xenon has been the subject of several interesting studies for a long time.¹⁻³ Whereas $4d$ photoionization has been studied both in nonrelativistic^{3,4} and relativistic² models, photoionization from $4p$ has been studied only in the nonrelativistic approximation.^{4,5} No relativistic many-body calculations on $4p$ and $4d$ photoionization in the vicinity of the Cooper minimum have been reported to our knowledge. Several interesting features were reported in the recent time-of-flight measurements of Xe $4p$ photoionization in the experiments done by Lindle *et al.*⁶ at the Stanford Synchrotron Radiation Laboratory. In particular, it was speculated in that work that $4p$ photoionization is influenced by photoionization channels from the $4d$ subshell.

In order to investigate the role of interchannel coupling between $4p$ and $4d$ photoionization channels we have made use of the relativistic random-phase approximation (RRPA) which takes into account major correlation effects.^{7,8} Furthermore, we have used the semiempirical procedure⁹⁻¹² of employing experimental removal energies⁶ rather than the Dirac-Fock eigenvalues for the $4p$ and $4d$ subshells. This procedure⁹ makes it possible to include in the calculation certain many-body effects which are omitted in the random-phase approximation (RPA). Specifically, we have done the following types of calculations in the photon energy range 160–325 eV.

(a) $4p$ and $4d$ photoionization done separately without coupling channels from $4p$ to those from $4d$. In this calculation, only intrashell correlations are therefore included via the five relativistic dipole channels from the $4p_{1/2}, 4p_{3/2}$ levels and the six channels from $4d_{3/2}, 4d_{5/2}$, respectively.

(b) An 11-channel calculation in which the above (5+6) channels were coupled with each other. The Dirac-Fock thresholds were replaced by the experimental thresholds to include some non-RPA (Refs. 9–12) corre-

lations in this calculation. The Dirac-Fock thresholds for $4p_{1/2}, 4p_{3/2}, 4d_{3/2}$, and $4d_{5/2}$ are 175.578, 162.797, 73.775, and 71.664 eV, respectively. The experimental $4p$ (spin-orbit-unresolved) threshold is at 145.5 eV. Half of the splitting between the Dirac-Fock $4p_{3/2}$ and $4p_{1/2}$ thresholds was added to and subtracted from the experimental $4p$ threshold of 145.5 eV in order to get the experimental thresholds for $4p_{1/2}$ and $4p_{3/2}$, respectively, and these were used in this calculation.

The separate (a) and (b) calculations clearly bring out the role of $4d$ influence on $4p$ photoionization in the region studied.

II. $4d$ SUBSHELL

The $4d$ subshell photoionization was previously studied in the RRPA by Huang, Johnson, and Cheng.² Huang *et al.* had coupled 13 dipole channels from the $5s, 5p$, and $4d$ subshells. As a result of this coupling, the oscillator strength in the $5p$ and $5s$ channels goes through a local maximum approximately at the energy at which $4d$ photoionization peaks at its “delayed maximum” due to the centrifugal barrier effect.^{13,14} This was experimentally verified.¹⁵ The $4d$ calculation of Huang *et al.* was limited to the photon energy range of ~ 75 – ~ 150 eV. The Cooper minimum in the $4d$ cross section as observed by the experiments of Lindle *et al.* was found to be beyond this energy range and has been studied in this calculation. The experimental data⁶ and the results of the present calculations [type (b) above, using experimental thresholds] are presented in Fig. 1. Since the experimental data do not correspond to the absolute cross sections, in order to compare our results, we have normalized the experimental data to the calculated cross section at 220 eV. The initial fall in the $4d$ cross section follows the tail end of a shape resonance.² The cross section is seen to go through a Cooper minimum^{13,14,16} at ~ 180 eV in excellent agreement with the experimental finding.⁶ In fact, in the entire photon energy region considered in this study the agreement between experimental data and the present calculation is very good.

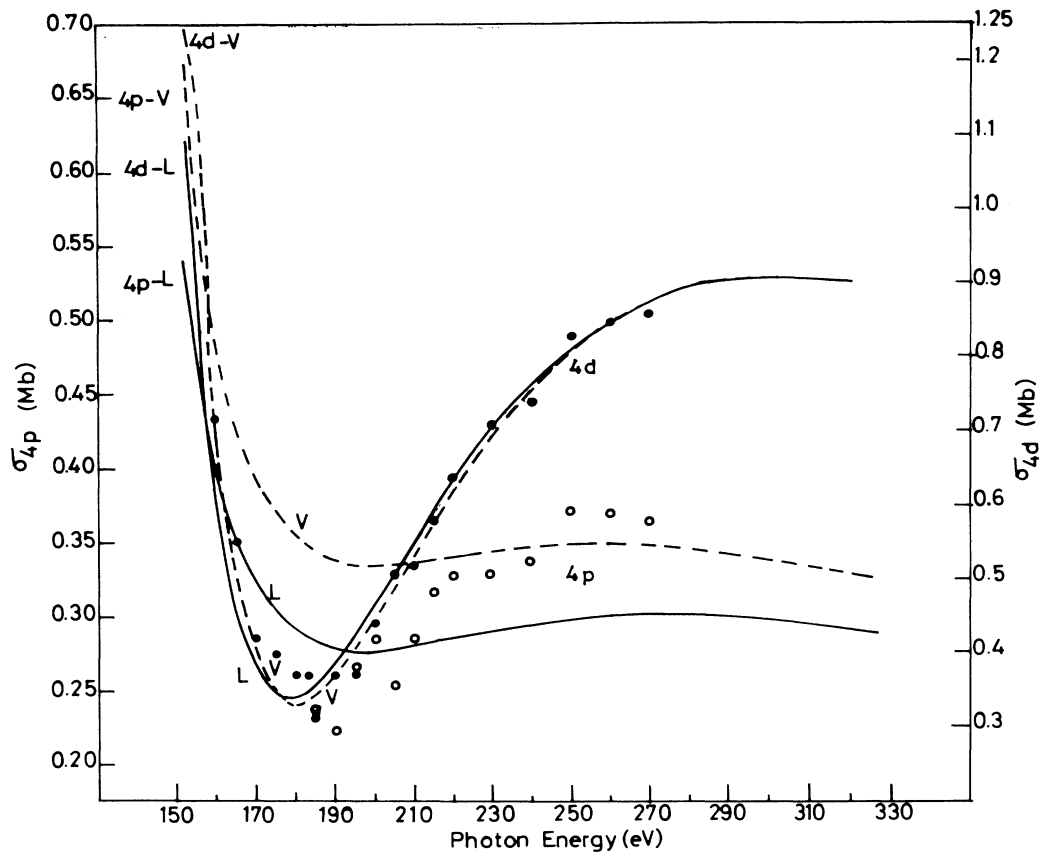


FIG. 1. $4d$ and $4p$ photoionization cross sections. Solid and dashed lines are for the length and velocity forms, respectively. Solid circles are the $4d$ experimental cross sections and the open circles are the $4p$ experimental cross sections from Ref. 6. Normalization of the experimental data is as per the discussion in the text.

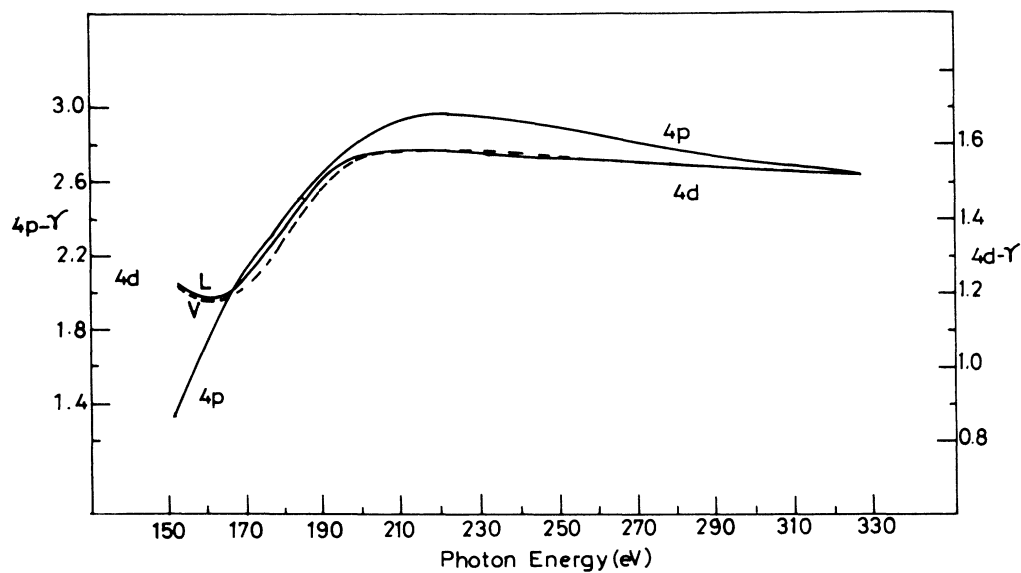


FIG. 2. $\sigma(4d_{5/2}):\sigma(4d_{3/2})$ branching ratio and $\sigma(4p_{3/2}):\sigma(4p_{1/2})$ branching ratio. The solid line and the dashed line correspond to the length and velocity form, respectively. The branching ratio for $4p$ is almost the same in both length and velocity forms.

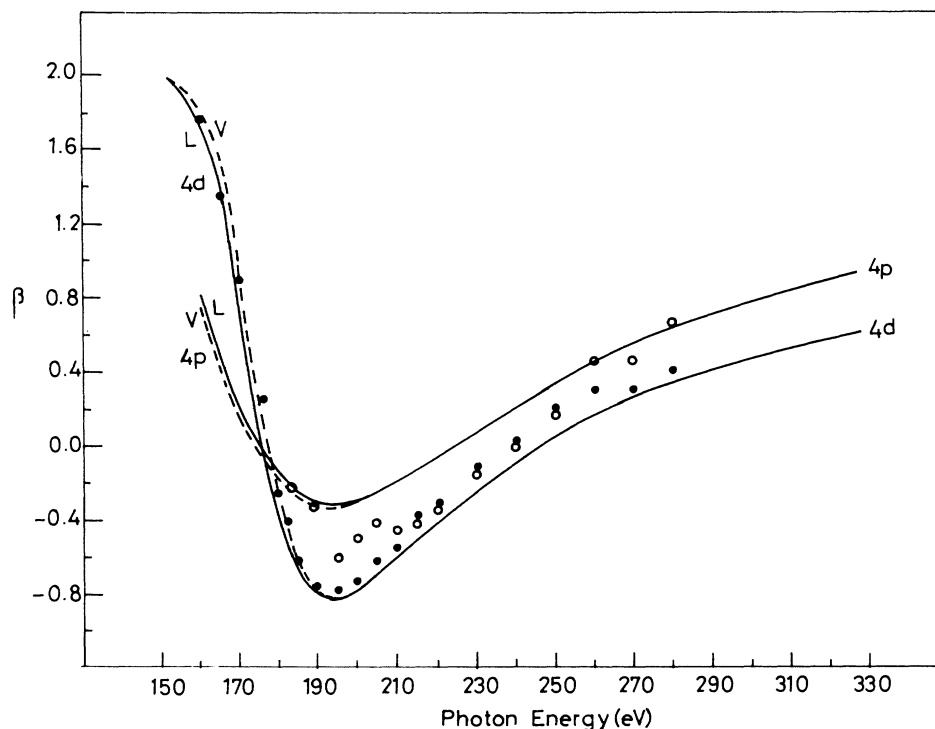


FIG. 3. Angular distribution asymmetry parameters for $4d$ and $4p$ subshells. Solid and dashed lines are length and velocity forms, respectively. Solid and open circles are the experimental data from Ref. 6 of $4d$ and $4p$ angular distribution asymmetry parameters, respectively.

The branching ratio for $4d_{5/2}:3d_{3/2}$ photoionization is shown in Fig. 2. The statistical value for this ratio is 1.5. Near the Cooper minimum in the cross section this ratio shows a dip which is due to the fact that $4d_{5/2}$ goes through its minimum at a lower photon energy than $4d_{3/2}$. This behavior is characteristic of the manner in which the Cooper minima in the relativistically split dipole channels occur, as for example in the case of Cooper minima in the $6p$ (Ref. 16) and $5d$ (Refs. 17 and 18) photoionization. A similar profile is seen in the vicinity of the $4d$ Cooper minimum in cadmium¹⁹ and palladium.²⁰ The value of γ subsequently rises above the statistical value, since the Cooper minimum in the channel originating from the $4d_{3/2}$ is at a higher photon energy. At still higher energies γ decreases and approaches its statistical value.

The angular distribution asymmetry parameter for xenon $4d$ photoionization is shown in Fig. 3. Also shown are the experimental data of Lindle *et al.*⁶ for the sake of comparison. The agreement between the experimental data and our calculation is excellent and the general profile is very similar to that of β for cadmium¹⁹ and palladium²⁰ $4d$ in the energy range following the Cooper minimum in their respective cross sections. We may add that the results of type-(a) calculation (not shown) for $4d$ do not differ very much from those of type (b). This is to be expected since the $4d$ channels are the dominant ones.

III. $4p$ SUBSHELL

As mentioned above, the $4p$ photoionization parameters were calculated by coupling only the five channels originating from this subshell [type (a)] and also by coupling [type (b)] these five channels to the six relativistic dipole channels from $4d$. The result shown in Fig. 1 for the $4p$ cross section corresponds to type (b). The experimental data⁶ for $4p$ photoionization have also been shown (as open circles) in Fig. 1. The experimental data shown in this figure are twice the values reported by Lindle *et al.*⁶ This has been done to place them in the vicinity of the calculated cross sections for the sake of comparison. For the purpose of Fig. 1, we have scaled the experimental data first by the same factor we employed for the experimental $4d$ cross sections, since the experimental data for $4d$ and $4p$ were on a common arbitrary scale. We then multiplied the resulting experimental cross sections by 2. It may be noted that the scaling of the experimental $4p$ measured values was based on a single prominent contribution to $4p$ photoionization.

The scaling procedure we have adopted in Fig. 1 should therefore be able to provide a basis for at least a qualitative understanding of the energy dependence of the $4p$ cross section in the context of the fact that the assignment of the experimental data to $4p$ photoionization was done with reference to a single configuration which

Lindle *et al.* considered to be the dominant one. The analysis of these results is complicated by the fact that the $4p_{3/2}$ and $4p_{1/2}$ hole states are degenerate with the Xe^+ ($4d^8 4f$) configuration which is not included in the RPA.⁶ The RRPA ground state picks up only those configurations that couple to the single configurational 1S_0 state. The limited agreement between the experimental data and the present calculations is, therefore, an indicator of how important the non-RPA configuration interactions are. It may be added that certain non-RPA correlations have been picked in the present calculation by employing the experimental thresholds instead of the Dirac-Fock thresholds. This procedure⁹⁻¹² marginally accentuated the appearance of the minimum in $4p$ cross section in response to coupling with the $4d$ channels compared to another calculation we did (not shown in Fig. 1) in which the Dirac-Fock thresholds were employed. The fact that the RRPA result for the $4p$ cross section goes through a minimum in the vicinity of the $4d$ Cooper minimum does, however, give credence to the fact that interchannel coupling with $4d$ channels plays a significant role in $4p$ photoionization. We confirmed this by decoupling the $4d$ photoionization channels and including only the intrashell correlations [type (a)]. The latter result (not shown in Fig. 1 to avoid crowding) does not show any such minimum; it is monotonically decreasing and is slightly higher than the result of the type-(b) calculation.

The profiles of the branching ratio $\sigma(4p_{3/2}):\sigma(4p_{1/2})$ (Fig. 2) and the angular distribution asymmetry parameter (Fig. 3) show²¹⁻²³ that the $4p$ Cooper minimum is in the discrete part of the spectrum. The results of our calculations for $4p$ β are in fair agreement with the experi-

mentally determined values, suggesting that RRPA does account for important features in $4p$ photoionization.

IV. CONCLUDING REMARKS

Lindle *et al.*⁶ had proposed two alternative interpretations of their measurements of the $4p$ peak. One of these regarded it as a $4d$ satellite associated with the $4d^8 4f$ configuration, and the other considered the interchannel coupling with photoionization channels from the $4d$ subshell. In the RRPA, the latter consideration is adequately incorporated and the present calculation does indeed clearly demonstrate the fact that $4p$ photoionization is influenced by interchannel coupling in the vicinity of the $4d$ Cooper minimum, as was also seen in the nonrelativistic random-phase approximation with exchange (RPAE) calculation.⁴ Lack of complete agreement with experimental data may, however, be due to non-RPA correlations.²⁴ The agreement between experimental data and present calculation of $4p$ β nevertheless suggests that RRPA accounts well for major features of $4p$ photoionization.

ACKNOWLEDGMENTS

These calculations were done by using the computer code developed by Professor W. R. Johnson. We are thankful to him for letting us use it. One of us (P.C.D.) is thankful to Professor S. T. Manson for helpful discussions. Another (N.S.) acknowledges support by the Indian Institute of Technology. Cooperation received at the Computer Centre, IIT, Madras, is also gratefully acknowledged.

¹G. Wendin, *Breakdown of the One-Electron Pictures in Photoelectron Spectra*, Vol. 45 of *Structure and Bonding* (Springer-Verlag, Berlin, 1981), p. 1.

²K. N. Huang, W. R. Johnson, and K. T. Cheng, *At. Data Nucl. Data Tables*, **26**, 33 (1981).

³Z. Altun, M. Kutzner, and H. P. Kelly, *Phys. Rev. A* **37**, 4671 (1988).

⁴M. Ya. Amusia and N. A. Cherepkov, *Case Stud. At. Phys.* **5**, 47 (1975).

⁵D. J. Kennedy and S. T. Manson, *Phys. Rev. A* **5**, 227 (1972).

⁶D. W. Lindle, T. A. Ferret, P. A. Heimann, and D. A. Shirley, *Phys. Rev. A* **37**, 3808 (1988).

⁷W. R. Johnson and C. D. Lin, *Phys. Rev. A* **20**, 964 (1979).

⁸W. R. Johnson, C. D. Lin, K. T. Cheng, and C. M. Lee, *Phys. Script.* **21**, 409 (1980).

⁹H. P. Kelly, *Adv. Theor. Phys.* **2**, 75 (1968).

¹⁰S. L. Carter and H. P. Kelly, *J. Phys. B* **11**, 2467 (1978).

¹¹W. R. Johnson, V. Radojevic, P. C. Deshmukh, and K. T. Cheng, *Phys. Rev. A* **25**, 337 (1982).

¹²V. Radojevic and W. R. Johnson, *J. Phys. B* **16**, 177 (1983).

¹³S. T. Manson and J. W. Cooper, *Phys. Rev.* **165**, 126 (1968).

¹⁴U. Fano and J. W. Cooper, *Rev. Mod. Phys.* **40**, 441 (1968).

¹⁵S. Southworth, U. Becker, C. M. Truesdale, P. H. Kobrin, D. Lindle, S. Owaki, and D. A. Shirley, *Phys. Rev. A* **28**, 261 (1983).

¹⁶J. W. Cooper, *Phys. Rev.* **128**, 681 (1962).

¹⁷P. C. Deshmukh, V. Radojevic, and S. T. Manson, *Phys. Lett. A* **117**, 293 (1986).

¹⁸P. C. Deshmukh, B. R. Tambe, and S. T. Manson, *Aust. J. Phys.* **39**, 679 (1986).

¹⁹W. R. Johnson, V. Radojevic, P. C. Deshmukh, and K. T. Cheng, *Phys. Rev. A* **25**, 337 (1982).

²⁰N. Shanthi and P. C. Deshmukh (unpublished).

²¹N. Shanthi, P. C. Deshmukh, and S. T. Manson, *Phys. Rev. A* **37**, 4720 (1988).

²²N. Shanthi, *J. Phys. B* **21**, L427 (1988).

²³S. T. Manson, *J. Electron Spectrosc. Relat. Phenom.* **1**, 413 (1972).

²⁴P. C. Deshmukh and S. T. Manson, *Phys. Rev. A* **32**, 3109 (1985).